

Direct Hydrogenation of Dinitrogen and Dioxygen via Eley–Rideal Reactions

Yunxi Yao and Konstantinos P. Giapis*

Abstract: Most Eley–Rideal abstraction reactions involve an energetic gas-phase atom reacting directly with a surface adsorbate to form a molecular product. Molecular projectiles are generally less reactive, may dissociate upon collision with the surface, and thus more difficult to prove that they can participate intact in abstraction reactions. Here we provide experimental evidence for direct reactions occurring between molecular N_2^+ and O_2^+ projectiles and surface-adsorbed D atoms in two steps: first, the two atoms of the diatomic molecule undergo consecutive collisions with a metal surface atom without bond rupture; and second, the rebounding molecule abstracts a surface D atom to form N_2D and O_2D intermediates, respectively, detected as ions. The kinematics of the collisional interaction confirms product formation by an Eley–Rideal reaction mechanism and accounts for inelastic energy losses commensurate with surface re-ionization. Such energetic hydrogenation of dinitrogen may provide facile activation of its triple bond as a first step towards bond cleavage.

The Eley–Rideal (ER) reaction mechanism describes direct reactions between energetic gas-phase projectiles and surface adsorbates.^[1–3] Although there are indications that ER reactions may participate in heterogeneous catalysis under thermal reaction conditions,^[4–6] finding direct evidence has been challenging. With the exception of the first demonstration of an ER reaction in the protonation of a very large molecule $[N(C_2H_4)_3N]$,^[7] most studies have been limited to atomic projectiles.^[2,3,8–13] Molecular projectiles may be less reactive or may undergo collision-induced dissociation, which renders their participation in ER reactions more difficult to prove. However, collisional energy transfer in combination with adsorbate abstraction from surfaces may enable intra-molecular excitation in diatomic projectiles with strong (double or triple) bonds, thus activating them and starting the process of bond rupture. As such, ER reactions may present an important first step in some catalytic processes, especially when internal or kinetic energy is available to participating molecules. Such energies are encountered in plasma processing^[14] and astrophysical environments,^[15]

where more exotic chemical dynamics may dominate. For example, ER reactions between N_2^+ or O_2^+ , and surface-adsorbed hydrogen atoms to form N_2H or O_2H ions or neutrals is important in interstellar media,^[16] the Martian ionosphere,^[17] but also in heavy-ion cancer therapy and space radiation exposure during missions.^[18]

N_2 activation is considered to be the first step towards $N\equiv N$ bond cleavage, occurring in the ammonia synthesis via the Haber–Bosch process, typically on catalytic surfaces under high temperature and pressure conditions.^[19,20] An alternative mechanism has been proposed, where activation of $N\equiv N$ occurs via partial hydrogenation to N_2H , without complete cleavage of the triple bond.^[21] This associative activation of N_2 attracted no interest despite similarities with the nitrogenase process.^[22] Here we report the observation of N_2D (and N_2H) intermediate, formed directly via an ER reaction between molecular N_2^+ projectiles and surface-adsorbed D (H) atoms, which lends credibility to the N_2 partial hydrogenation pathway, albeit at hyperthermal kinetic energies. Likewise, observation of O_2D , formed by ER reactions between molecular O_2^+ and adsorbed D, also demonstrates O_2 activation through partial hydrogenation of the $O=O$ bond, bypassing the requirement for O_2 dissociation. O_2H is an important reaction intermediate in H_2O_2 synthesis.^[23]

The direct surface reaction between N_2^+ projectiles and adsorbed D was first studied on a polycrystalline Pd surface, denoted as Pd(D). Figure 1 a,b show scattered N_2^+ and N_2D^+ ion energy distributions from $N_2^+/Pd(D)$ at an incidence energy of $E_0 = 97.3$ eV. For these experiments, the D_2 background pressure was varied between zero and 1×10^{-7} torr.

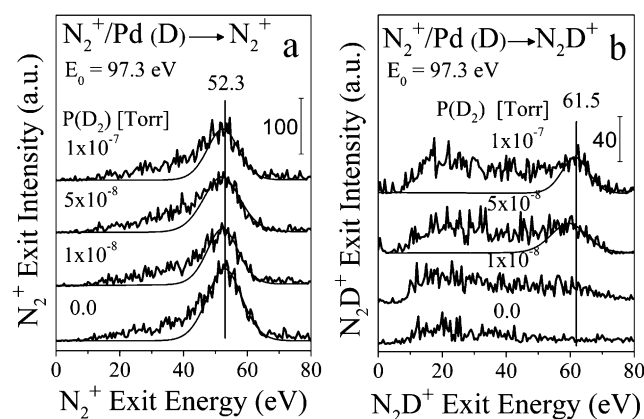


Figure 1. Energy distributions for: a) N_2^+ and b) N_2D^+ ion exits from $N_2^+/Pd(D)$ at $E_0 = 97.3$ eV as a function of the D_2 background pressure. Gaussian fittings are used to locate the dynamic peak energy. Note the sputtering contribution to N_2D^+ signal at an exit energy of 20 eV.

[*] Dr. Y. X. Yao, Prof. K. P. Giapis
Division of Chemistry and Chemical Engineering
California Institute of Technology
Pasadena, CA 91125 (USA)
E-mail: giapis@cheme.caltech.edu
Homepage: <http://cheme.che.caltech.edu/groups/kpg/index.html>

Supporting information and the ORCID identification number(s) for the author(s) of this article can be found under <http://dx.doi.org/10.1002/anie.201604899>.

On the *clean* Pd surface, a N_2^+ scattering peak is observed at 52.3 eV. Upon D_2 exposure, a new peak appears at 61.5 eV, corresponding to 30 amu/e (N_2D^+), whose intensity increases with D_2 pressure. Clearly, the N_2D product is formed dynamically by N_2^+ projectiles after the addition of D atoms to the surface. Note that N^+ and ND^+ are also detected (Figure S1 in the Supporting Information), albeit due to sputtering (forced ejection of surface species).

The dynamics of the direct surface reaction between N_2^+ projectiles and adsorbed D atoms is revealed by varying the incidence energy E_0 (Figure 2a,b). Both N_2^+ and N_2D^+ scattering peaks shift rapidly to higher energies with E_0 , which suggests that the fast N_2D^+ product formation is dynamic, an indication of an ER reaction.^[24] Note that the N_2D^+ peak dies out above 100 eV. In contrast, the position of the much broader N^+ and ND^+ peaks varies only slightly with N_2^+ incidence energy, characteristic of sputtering products (Figure S2).

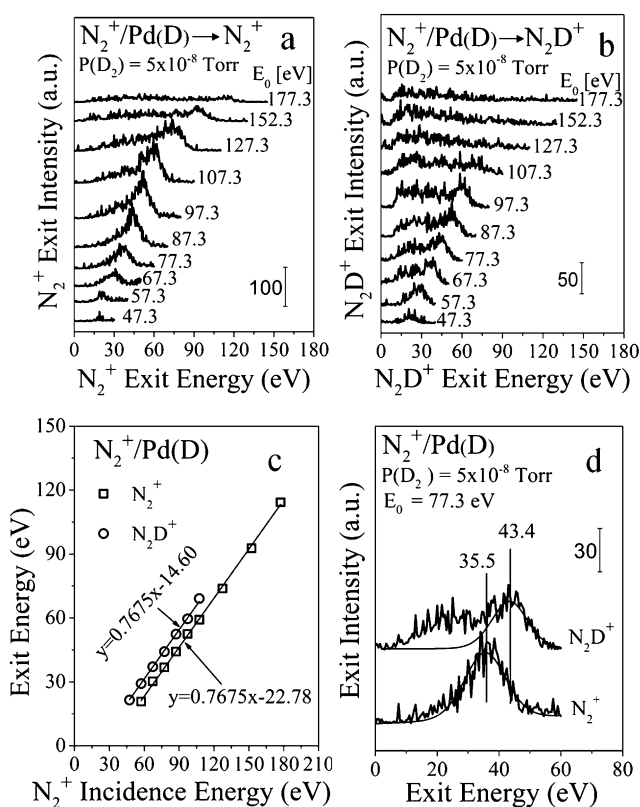


Figure 2. Energy distributions for: a) N_2^+ and b) N_2D^+ ion exits from $\text{N}_2^+/\text{Pd}(\text{D})$ as a function of the N_2^+ incidence energy, in a background of 5×10^{-8} torr D_2 . c) Peak exit energies of N_2^+ and N_2D^+ as a function of incidence energy. d) Comparison of dynamic peak energies for N_2^+ and N_2D^+ ion exits at $E_0 = 77.3$ eV.

The kinetic energies of the fast N_2^+ and N_2D^+ products are plotted in Figure 2c as a function of E_0 . Both sets of data exhibit linear dependence. The N_2^+ exit energy can be predicted assuming binary surface collisions between each N atom of the N_2^+ projectile bouncing off consecutively on a Pd atom. Thus, the kinematic factor for N_2^+ exiting the Pd

surface at a scattering angle of 90° is calculated from the Baule formula for two N atoms colliding individually one after the other with the same Pd atom. We obtain a value of 0.7675, which captures remarkably well the slope of the N_2^+ exit energy data. The one-parameter linear fitting yields a negative intercept of 22.78 eV, corresponding to inelastic energy loss associated with N_2^+ surface interaction. Meanwhile, the N_2D^+ exit data can also be fitted well with the same kinematic factor of 0.7675 (for N_2^+ ion exits), suggesting that the N_2D^+ exit energy is mainly determined by the surface collision between N_2^+ projectiles and Pd atoms. As conjectured for single-atom abstraction reactions,^[24] a transient state forms between the incoming N_2^+ projectile, the Pd surface atom and the adsorbed D atom at the distance of closest approach, followed up by rebound of the molecular product $\text{N}_2\text{--D}$. Owing to the light mass of D atoms, the kinetic energy of the N_2D is approximately equal to that of the scattered N_2 . Ion scattering experiments on metal surfaces have established that ions are efficiently neutralized on the incoming path.^[25] Thus, most of the N_2^+ projectiles are converted into N_2 before the hard collision with the surface. Thus, N_2D formation can be attributed to ER reactions between *neutralized* N_2 projectiles and adsorbed D atoms. When ions (N_2^+ and N_2D^+) are observed exiting the surface, they must be formed by charge exchange with the surface either during the hard collision or on the outgoing trajectory. Surface re-ionization consumes energy, which leads to inelastic energy loss for the scattered product. Additional energy loss processes (e.g., electronic friction, internal excitations) further decrease the kinetic energy of the scattered product. The intercept of the linear fittings of Figure 2c is a measure of the total inelastic energy loss incurred during the scattering process, which is termed “inelasticity”. For N_2^+ ion exits, the inelasticity is 22.78 eV, which is larger than the ionization energy (IE) of N_2 (15.58 eV)^[26] as expected. The inelasticity for N_2D^+ is 14.60 eV, which is also larger than the IE of N_2D (7.92 eV).^[27] The inelasticity difference between N_2^+ and N_2D^+ is 8.18 eV, remarkably close to the energy difference of 7.66 eV between the IEs of N_2 and N_2D . This result is not fortuitous: since the neutralized projectile is the common precursor to the N_2^+ and N_2D^+ products, any *additional* inelastic losses beyond ionization are expected to be very similar. This analysis is validated in Figure 2d by comparing the energy distributions of N_2^+ and N_2D^+ at $E_0 = 77.3$ eV: the fast N_2D^+ and N_2^+ peaks appear at 43.4 and 35.5 eV, respectively, yielding a difference in kinetic energy of 7.9 eV.

ER reactions between N_2^+ projectiles and adsorbed H atoms on Pd exhibit similar behavior to $\text{N}_2^+/\text{Pd}(\text{D})$ (Figure S3). The N_2H^+ product exits the surface with kinetic energy circa 8 eV larger than that of N_2^+ , again very close to the ionization energy difference between N_2 and N_2H . Thus, no isotope effect is observed in N_2^+ reactions with adsorbed D or H atoms on Pd.

The role of the surface in ER reactions between N_2^+ projectiles and adsorbed D atoms was further investigated by performing scattering experiments on polycrystalline Pt surfaces. Again, N_2D^+ products emerge immediately upon exposure of the Pt sample to D_2 . Figure 3a,b show energy distributions of scattered N_2^+ and N_2D^+ from $\text{N}_2^+/\text{Pt}(\text{D})$ in

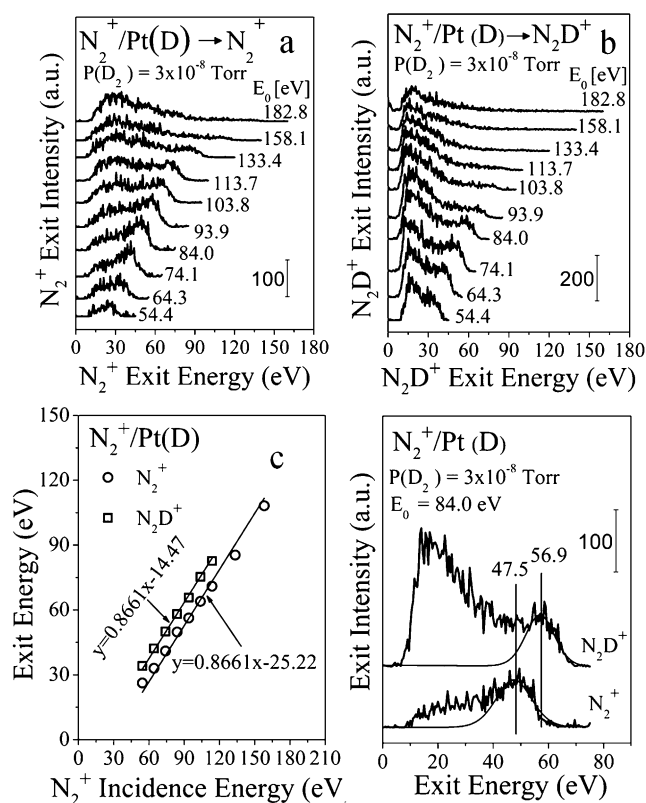


Figure 3. Energy distributions for: a) N_2^+ and b) N_2D^+ ion exits from $N_2^+/Pt(D)$ as a function of the N_2^+ incidence energy, in a background of 3×10^{-8} torr D_2 . c) Peak exit energies of N_2^+ and N_2D^+ as a function of incidence energy. d) Comparison of dynamic peak energies for N_2^+ and N_2D^+ ion exits at $E_0 = 84.0$ eV.

a background of 3×10^{-8} torr D_2 at various incidence energies. Fast exit peaks for both N_2^+ and N_2D^+ are observed as before. In contrast to Pd, however, scattering on Pt produces a much stronger N_2D^+ peak at 20 eV, evidence that the indirect channel (sputtering) is more significant. This observation suggests that more N_2D is trapped on the Pt surface. Since a Langmuir–Hinshelwood reaction between N_2 and adsorbed D is unlikely at room temperature,^[28] how does N_2D come to exist on the surface and why is there more sputtering signal on the Pt vs. Pd surface? First, we attribute trapped N_2D to hot atom reactions.^[29] Neutralized incident N_2 molecules may undergo multiple bounces on the rough surface losing most, but not all, of their kinetic energy before abstracting D atoms. Thus formed N_2D can become trapped and give rise to a slow peak in the energy distributions upon sputtering by the incident beam. Second, it is possible that N_2D adsorbs stronger on Pt vs. Pd, thus increasing coverage and producing stronger sputtering signal. We could not find any measurements for N_2D adsorption energies to confirm this effect. However, the same effect is seen for N_2^+ scattering on Pt(H) vs. Pd(H): The indirect N_2H^+ peak is much more pronounced on the former surface. Howalt et al.^[30] calculated adsorption energies of N_2H on metal nanoclusters (using DFT), confirming the stronger adsorption on Pt vs. Pd.

The peak energies of the dynamic N_2^+ and N_2D^+ products, plotted in Figure 3c as a function of N_2^+ incidence energy,

exhibit linear dependence and can be fitted well with a kinematic factor of 0.8661, calculated for two sequential N atom collisions with Pt. The inelasticity for scattered N_2^+ is 25.22 eV versus 14.47 eV for N_2D^+ , which yields an inelasticity difference of 10.75 eV, somewhat larger than the difference in ionization energies between N_2 and N_2D . This value is close to 9.4 eV obtained from a comparison of the exit energy distributions for N_2D^+ and N_2^+ at $E_0 = 84.0$ eV (Figure 3d).

Thus, the heavier Pt surface affects both the elastic energy transfer and the trapping of molecular N_2 and N_2D . However, the dynamic scattering behavior of the N_2D^+ product is similar to that seen on Pd: Its kinetic energy is determined by the N_2/Pt surface collision, reduced by somewhat larger inelastic losses. The N_2D^+ product possesses larger kinetic energy than unreacted N_2^+ , by an amount close to the ionization energy difference between N_2 and N_2D , which again confirms that the detected ions are produced by surface re-ionization. Sputtered ND^+ is also observed for $N_2^+/Pt(D)$ for the same reasons as on Pd(D) (Figure S4). Scattering experiments with adsorbed H yield the expected N_2H^+ ER product, with identical dynamic behavior as N_2D^+ (Figure S5).

The generic nature of the ER abstraction reactions for diatomic projectiles is further verified for molecular O_2^+ scattering on Pd and Pt surfaces, covered with D atoms. In addition to O_2^+ , scattered O_2^- is also observed for O_2^+ scattering on *clean* Pt. Upon exposure to D_2 , a weak O_2D^+ peak is observed, accompanied with much stronger OD^+ and OD^- products (Figure S6, S7). The observation of O_2D^+ suggests that the O=O double bond can also be activated by partial hydrogenation. Energy distributions of scattered O_2^+ , O_2^- and O_2D^+ are shown in Figure 4a–c, as a function of incidence energy for $O_2^+/Pt(D)$ in a background of 1×10^{-7} torr D_2 .

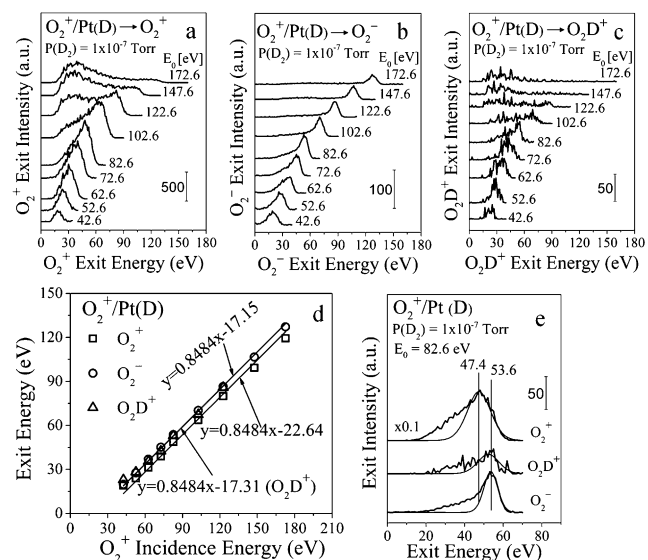


Figure 4. Energy distributions for: a) O_2^+ , b) O_2^- and c) O_2D^+ ion exits from $O_2^+/Pt(D)$ as a function of the N_2^+ incidence energy, in a background of 1×10^{-7} torr D_2 . d) Peak exit energies of O_2^+ , O_2^- and O_2D^+ as a function of O_2^+ incidence energy. e) Comparison of dynamic peak energies for O_2^+ , O_2^- and O_2D^+ ion exits at $E_0 = 82.6$ eV.

10^{-7} torr D_2 . For all dynamically scattered products, the exit energy data, plotted in Figure 4d, depend linearly on the O_2^+ incidence energy and can be fitted well with a kinematic factor of 0.8484, calculated for two sequential O atom collisions with Pt. The ion exit energy of O_2D^+ is almost equal to that of O_2^- , and both are larger than that of O_2^+ . This is further confirmed in Figure 4e by comparing energy distributions for scattered O_2^+ , O_2^- and O_2D^+ from $O_2^+/Pt(D)$ at $E_0 = 82.6$ eV.

The difference in kinetic energies between O_2^+ and O_2^- can be easily explained by different surface ionization mechanisms for neutral O_2 . The scattered O_2^- is formed by resonant electron transfer from the surface, while O_2^+ is formed by direct ionization during the hard collision, which is energetically more expensive.^[31] An energy barrier of $\phi - S = 5.19$ eV has to be overcome to form O_2^- , where ϕ is the surface work function of Pt (5.64 eV),^[32] and S is the electron affinity of O_2 (0.45 eV).^[33] Direct ionization to form O_2^+ requires at least the IE of O_2 (12.07 eV).^[34] Thus, this argument predicts a difference of 6.88 eV ($IE - \phi + S$) between O_2^- and O_2^+ exit energies, with the positive ion being slower. This value is close to 6.2 eV inferred from Figure 4e and in agreement with the inelasticity difference of 5.49 eV between O_2^+ (22.64 eV) and O_2^- (17.15 eV) inferred from the fittings of Figure 4d.

It is interesting to note why O_2D^+ ions exit faster than O_2^+ . Indeed, the exit energy of O_2D^+ is about 5.33 eV larger than O_2^+ , though the IE of O_2D is 11.35 eV,^[35] which is only 0.72 eV lower than the IE of O_2 . The O_2D^+ ion must therefore form by a different mechanism than direct ionization. Resonant ionization of O_2D with an electron transfer to the surface has an energy barrier of 6.16 eV ($\phi - IE$), which is very close to the energy penalty for forming O_2^- (5.19 eV). Thus, surface resonant ionization of O_2D can explain the larger exit energy of O_2D^+ vs. O_2^+ , and its appearance at the same energy as O_2^- .

In summary, direct ER abstraction reactions have been demonstrated in single-collisions of diatomic molecular ions (N_2^+ , O_2^+) and adsorbed D(H) atoms. The kinetic energies of the products (N_2D^+ , O_2D^+) depend linearly on the incidence energy, and can be predicted by simple kinematics, minus inelastic losses mainly from surface re-ionization. In addition to facilitating neutralization and re-ionization, the role of the surface is to slow down the projectile so that it can bond with the adsorbate. The direct formation of N_2D^+ and O_2D^+ demonstrates activation of N_2 and O_2 bonds through partial hydrogenation in energetic collisions with surfaces.

Experimental Section

All experiments were carried out in a custom-built ultra-high vacuum (UHV) scattering apparatus, equipped with a low energy ion beam-line connected to an inductively coupled plasma ion source.^[12,36,37] Molecular N_2^+ and O_2^+ ions were mass selected from the plasma discharge, operated at 5 mTorr and 500 W, with a feed of $N_2/Ar/Ne$ and $O_2/Ar/Ne$, respectively. Typical beam current for N_2^+ was 10–27 μA , and for O_2^+ was 7–17 μA , over a spot 3 mm in diameter. A fixed 90° lab scattering angle was used for all experiments, with the ion beam delivered to the surface at 45° angle of incidence. Surface-adsorbed D atoms were produced by in situ dosing with D_2 through

a pipe situated 2 cm from the sample surface, kept at room temperature. D_2 was chosen to avoid interference with background H_2 from the UHV chamber. Polycrystalline Pd and Pt samples were employed as scattering targets; the surfaces were cleaned in situ with an Ar^+ ion gun prior to each scattering experiment. Products were energy- and mass-resolved using a 90° hemispherical energy analyzer followed up by a quadrupole mass spectrometer. An appropriately biased channeltron was used in pulse-counting mode to detect positive and negative ions exciting the quadrupole.

Acknowledgements

Funding support from the National Science Foundation is gratefully acknowledged (award number 1202567).

Keywords: Eley–Rideal reactions · hydroperoxyl · ion scattering · nitrogen activation · surface dynamics

How to cite: *Angew. Chem. Int. Ed.* **2016**, 55, 11595–11599
Angew. Chem. **2016**, 128, 11767–11771

- [1] K. R. Lykke, B. D. Kay in *Laser Photoionization and Desorption Surface Analysis Techniques*, Vol. 1208 (Ed.: N. S. Nogar), SPIE, Bellingham, **1990**, p. 18.
- [2] C. T. Rettner, D. J. Auerbach, *Science* **1994**, 263, 365–367.
- [3] W. H. Weinberg, *Acc. Chem. Res.* **1996**, 29, 479–487.
- [4] C. H. F. Peden, D. W. Goodman, M. D. Weisel, F. M. Hoffmann, *Surf. Sci.* **1991**, 253, 44–58.
- [5] A. Bongiorno, U. Landman, *Phys. Rev. Lett.* **2005**, 95, 106102.
- [6] H. J. Freund, G. Meijer, M. Scheffler, R. Schlögl, M. Wolf, *Angew. Chem. Int. Ed.* **2011**, 50, 10064–10094; *Angew. Chem.* **2011**, 123, 10242–10275.
- [7] E. W. Kuipers, A. Vardi, A. Danon, A. Amirav, *Phys. Rev. Lett.* **1991**, 66, 116–119.
- [8] C. T. Rettner, D. J. Auerbach, *Phys. Rev. Lett.* **1995**, 74, 4551–4554.
- [9] C. L. Quinteros, T. Tzvetkov, D. C. Jacobs, *J. Chem. Phys.* **2000**, 113, 5119–5122.
- [10] B. Jackson, D. Lemoine, *J. Chem. Phys.* **2001**, 114, 474–482.
- [11] B. Jackson, X. Sha, Z. B. Guvenc, *J. Chem. Phys.* **2002**, 116, 2599–2608.
- [12] M. J. Gordon, X. Qin, A. Kutana, K. P. Giapis, *J. Am. Chem. Soc.* **2009**, 131, 1927–1930.
- [13] T. Zaharia, A. W. Kleyn, M. A. Gleeson, *Phys. Rev. Lett.* **2014**, 113, 053201.
- [14] R. Masel in *Principles of Adsorption and Reaction on Solid Surfaces*, Wiley, New York, **1996**, pp. 444–448.
- [15] H. Nilsson, G. S. Wieser, E. Behar, C. S. Wedlund, E. Kallio, H. Gunell, N. J. T. Edberg, A. I. Eriksson, M. Yamauchi, C. Koenders, M. Wieser, R. Lundin, S. Barabash, K. Mandt, J. L. Burch, R. Goldstein, P. Mokashi, C. Carr, E. Cupido, P. T. Fox, K. Szego, Z. Nemeth, A. Fedorov, J. A. Sauvand, H. Koskinen, I. Richter, J. P. Lebreton, P. Henri, M. Volwerk, C. Vallat, B. Geiger, *Astron. Astrophys.* **2015**, 583, A20.
- [16] D. C. Knauth, B. G. Andersson, S. R. McCandliss, H. W. Moos, *Nature* **2004**, 429, 636–638.
- [17] J. L. Fox, *Icarus* **2015**, 252, 366–392.
- [18] Z. Deng, I. Bald, E. Illenberger, M. A. Huels, *Angew. Chem. Int. Ed.* **2008**, 47, 9509–9512; *Angew. Chem.* **2008**, 120, 9651–9654.
- [19] G. Ertl, *Angew. Chem. Int. Ed.* **2008**, 47, 3524–35354; *Angew. Chem.* **2008**, 120, 3578–3590.
- [20] S. Dahl, A. Logadottir, R. C. Egeberg, J. H. Larsen, I. Chorkendorff, E. Törnqvist, J. K. Nørskov, *Phys. Rev. Lett.* **1999**, 83, 1814–1817.
- [21] S. Carrà, R. Ugo, *J. Catal.* **1969**, 15, 435–438.

- [22] H. J. Himmel, M. Reiher, *Angew. Chem. Int. Ed.* **2006**, *45*, 6264–6288; *Angew. Chem.* **2006**, *118*, 6412–6437.
- [23] S. Siahrostami, A. Verdaguer-Casadevall, M. Karamad, D. Deiana, P. Malacrida, B. Wickman, M. Escudero-Escribano, E. A. Paoli, R. Frydendal, T. W. Hansen, I. Chorkendorff, I. E. L. Stephens, J. Rossmeisl, *Nat. Mater.* **2013**, *12*, 1137–1143.
- [24] Y. Yao, K. P. Giapis, *Phys. Rev. Lett.* **2016**, *116*, 253202.
- [25] D. C. Jacobs, *Annu. Rev. Phys. Chem.* **2002**, *53*, 379–407.
- [26] T. Trickl, E. F. Cromwell, Y. T. Lee, A. H. Kung, *J. Chem. Phys.* **1989**, *91*, 6006–6012.
- [27] A. Quinto-Hernandez, A. M. Wodtke, Y. Y. Lee, T. P. Huang, W. C. Pan, J. J. M. Lin, *J. Phys. Chem. A* **2009**, *113*, 3822–3829.
- [28] K. Honkala, A. Hellman, I. N. Remediakis, A. Logadottir, A. Carlsson, S. Dahl, C. H. Christensen, J. K. Nørskov, *Science* **2005**, *307*, 555–558.
- [29] J. Harris, B. Kasemo, *Surf. Sci.* **1981**, *105*, L281.
- [30] J. G. Howalt, T. Bligaard, J. Rossmeisl, T. Vegge, *Phys. Chem. Chem. Phys.* **2013**, *15*, 7785–7795.
- [31] K. Golibrzuch, N. Bartels, D. J. Auerbach, A. M. Wodtke, *Annu. Rev. Phys. Chem.* **2015**, *66*, 399–425.
- [32] Electron work function of the elements. In CRC Handbook of Chemistry and Physics, 96th ed, 2015–2016. <http://www.hbcpnetbase.com>.
- [33] K. M. Ervin, I. Anusiewicz, P. Skurski, J. Simons, W. C. Lineberger, *J. Phys. Chem. A* **2003**, *107*, 8521–8529.
- [34] R. G. Tonkyn, J. W. Winniczek, M. G. White, *Chem. Phys. Lett.* **1989**, *164*, 137–142.
- [35] J. M. Dyke, N. B. H. Jonathan, A. Morris, M. J. Winter, *Mol. Phys.* **1981**, *44*, 1059–1066.
- [36] J. Mace, M. J. Gordon, K. P. Giapis, *Phys. Rev. Lett.* **2006**, *97*, 257603.
- [37] Y. Yao, K. P. Giapis, *ChemPhysChem* **2016**, *17*, 1430–1434.

Received: May 19, 2016

Revised: July 5, 2016

Published online: August 18, 2016